

Mechanical properties and microstructural investigation of polypropylene/exfoliated graphite nanoplatelets/nano-magnesium oxide composites

A. I. Alateyah ^{1*}, F. H. Latief ²

¹ Qassim University, Unaizah Engineering College, Qassim, Kingdom of Saudi Arabia

² Department of Mechanical Engineering, Al Imam Mohammad Ibn Saud Islamic University (IMSIU), PO. BOX 5701, Riyadh 11432, Kingdom of Saudi Arabia

*Corresponding author E-mail: aialateyah@gmail.com

Abstract

Polypropylene/exfoliated graphite nanoplatelets composites reinforced with a low concentration of nano-magnesia have been successfully fabricated, using injection molding machine. The mechanical properties and microstructure of the composites were investigated, in the present study. The XRD patterns of the composites showed the peaks of xGnP and n-MgO, where the intensity of the xGnP peaks became stronger with increasing the concentration of xGnP added into polypropylene matrix. In addition, the SEM micrographs revealed a good dispersion of fillers within the matrix. The results showed that increasing the amount of exfoliated graphite nanoplatelets up to 10 wt. % resulted in increasing the composite flexural strength, flexural modulus, and hardness up to 35% and 91%, 6.7%, respectively, compared to the monolithic polypropylene.

Keywords: Polypropylene; Exfoliated Graphite Nano platelets; Magnesium Oxide Nanoparticles; Mechanical Prop-erties; XRD; and SEM.

1. Introduction

Thermoplastic composites are distinguished with having many advantages over classical thermoset-based matrices composites, which could include the lightweight, processing easiness, extraordinary potential of recyclability, and minimum cost [1-6]. Polypropylene (PP) is one kind of broadly adopted thermoplastic resins, which have been utilized in extremely large scale in industrial applications such as non-structural uses, packaging, and automotive [7]. The extension of the wide utilization of PP was to find appropriate reinforcement techniques to ameliorate its properties, which was reflected in newly obtained matrices, such as carbon black [8], graphite [9], carbon nanotubes [10].

Lately, an introduction of new promising types of reinforcements, such as the exfoliated graphite nanoplatelets (xGnPs), resulted in obtaining outstanding properties for these matrices [11-16]. xGnPs are notable for having a semi-metallic character, which commonly comprises less than 10 layers of graphene, consequently, the resulted thickness does not exceed a few nanometers, while the other two dimensions could reach up to few 100 μm [17]. Therefore, xGnP is considered a supreme reinforcing material, which enhances the thermal, mechanical and electrical properties of the polymeric matrix [18], [19].

Moreover, other additions to the reinforced PP-based composites could include the magnesia nanoparticles (n-MgOs). n-MgOs are widely utilized metal oxides, which can be easily synthesized using inexpensive raw materials such as brines, magnesium salts and bearing minerals [20]. MgOs are usually selected to be used due to its superior properties such as high strength and modulus, melting point, hardness, and exceptional thermodynamic stability. As a result, MgO is chosen to be adopted as a suitable filler for

this work [21]. Up to now, very limited work has been carried out on MgO as a nano-filler added into PP-xGnP composites. Therefore, the aim of this work is to investigate the mechanical properties of PP/xGnP/n-MgO composites. Noted that the concentration of n-MgO used in this study was constant that is 2 wt. %, whereas the concentration of xGnP was varied from 0 to 10 wt. %.

2. Experimental procedures and methods

2.1. Materials

Filler materials used in this work, consisting of n-MgO and xGnP with a purity of 99.9%, were supplied by Tritrust Industrial Co, China. The average particle size of n-MgOs was 100 nm whereas the particle size and the thickness of xGnP were 10 μm and 5 nm, respectively. For the matrix, PP in granules shape was provided by SABIC, Kingdom of Saudi Arabia.

2.2. Fabrication of composites

In the present work, the process starts with weighing the PP, xGnP and n-MgOs, with fixed compositions, using an analytical balance, as presented in Table 1.

Table 1: Composition of Composites (All in Weight %).

Sample	PP (wt.%)	xGnPs (wt.%)	n-MgO (wt.%)
1	100	0	0
2	97	1	2
3	95.5	2.5	2
4	93	5	2
5	88	10	2

The weighed powders were mixed using a mechanical disperser, to obtain a homogeneous state for sometimes. Consequently, the mixed powders were put into a Battenfeld HM 1000/750 injection molding machine to produce the samples. Injection molding was carried out using L/D ratio 22, Screw diameter 45 mm, a clamping force of 10 tons, barrel and nozzle temperature of 230°C, pressure of 3000 psi, and mold temperature of 20°C. Five different sample compositions, presented in Table 1, were examined to investigate the effect on mechanical properties of PP-xGnP composites with the addition of n-MgOs.

2.2. Characterization

2.3.1. X-Ray diffraction analysis

X-ray diffraction (XRD) was used to confirm the composition of the nanocomposites and to determine the existing phases of the composites. Wide-angle X-ray diffraction (WAXD) patterns, which provide the characteristics of nanoparticles, were obtained with an X-ray diffractometer equipped with a CuK α radiation. Survey scan was run between 10° and 90°, with a scanning speed of 2° per minute.

2.3.2 Flexural test

The flexural properties, strength and modulus, of the PP for the corresponding samples of composites were examined using the 3-points bending test process, following the British-Adopted European Standard BS EN 2747:1998 [22]. The specimens were prepared by injection molding in rectangular cross-section specimens (54 mm \times 13 mm \times 3 mm. A span of 48 mm length was adopted using a 30 kN load cell, which was applied midway between the supports. The crosshead speed was set at 2 mm/minute, where all samples were loaded up to failure and then their average values were calculated.

2.3.3 Hardness measurement

The hardness method is based on the penetration of a specific type of indenter when forced into the material under specified conditions. The indentation hardness is inversely related to the penetration and is dependent on the elastic modulus and viscoelastic behavior of the material. The geometry of the indenter and the applied force influence the measurements such that no simple relationship exists between the measurements obtained with one type of durometer and those obtained with another type of durometer or other instruments used for measuring hardness. Hardness tests were carried out to measure shore D hardness using a Bareiss Shore Hardness Tester (DigiTestII) and in accordance with ASTM D2240-10 for a 6 mm thickness samples. Five time measurements were taken for each composition and then averaged.

2.3.4. Scanning electron microscopy (SEM)

The samples were prepared by fracturing (cryo- fracturing) the sample cutting 1 cm long pieces, from the neck portion of tensile samples, and attaching it to a 12.5 mm diameter Al stubs, having sticky 12 mm diameter C tabs. The samples were Au-Pd sputter coated for 1-2 minutes, at a deposition current of 25 mA, and partial pressure of ~0.1 torr for Ar. The samples were then transferred to be examined by SEM, following the setup shown in Table 2.

Table 2: Setup Conditions of SEM Used for Microstructural Observation.

Instrument	HV, kV	WD, mm	Spot Size	Image Modes	Image Resolution
FEI Quanta 200 (SEM-2)	20.0	15-25	3.0	SEI	1024 x 784

3. Results and discussions

3.1. X-Ray diffraction analysis

Wide Angle X-ray Diffraction (WAXD) is a widely adopted technique in the study of intercalation or exfoliation, which has the advantage of composites characterization. X-ray diffraction is used to explain the intercalation or exfoliation structures through utilizing methods for the inter-gallery spacing calculations, which are responsible for the recognition of the composites structures [22]. Using this technique in this section will be useful in identifying and presenting the amount of d-spacing of the inter-gallery for different particles loading composites; as well as, for neat polymer. Figure 1 shows the XRD patterns of the neat PP and PP/xGnP composites with various compositions of fillers. From the XRD patterns obtained, xGnP and n-MgO were found in samples 2 to 5, as shown in Figure 1. It is obviously seen that the xGnP peaks were detected in the two theta of 26.6° in all composite samples and this is fit to previous published report [23]. Meanwhile, the n-MgO was observed at the two theta of 42.9°, which is a straight suggestion for the face centered cubic crystalline phase (JCPDS No 45-0496) [24]. In addition, the intensity of the xGnP peaks became stronger with increasing the concentration of xGnP added into PP matrix whereas the intensity of n-MgO was relatively persistent as can be seen in Figure 1. Table 3 represents the change of the basal spacing (d_{001} spacing) of the composites, which were calculated by Bragg's Law using the values extracted from the XRD patterns according to [25]:

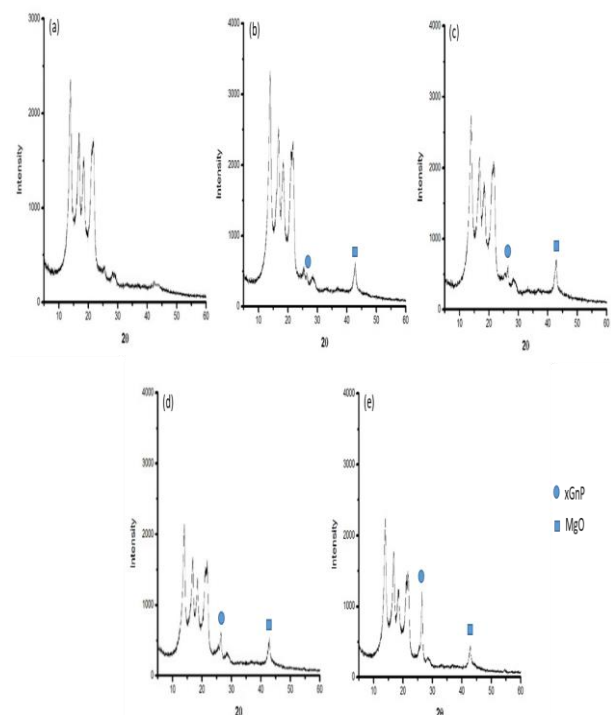


Fig. 1: XRD Curves of PP and Its Composites: (A) 100 Wt. % PP, (B) PP/ 1xgnp/2n-Mgo, (C) PP/ 2.5xgnp/2n-Mgo, (D) PP/ 5xgnp/2n-Mgo and (E) PP/ 10xgnp/2n-Mgo.

Table 3: XRD D-Spacing of Various PP and It's Nanocomposites Samples.

Samples	2 Theta	d-spacing [Å]
100 wt. % PP	21.87	4.06
PP/ 1xGnP/2n-MgO	21.03	4.22
PP/ 2.5xGnP/2n-MgO	21.11	4.21
PP/ 5xGnP/2n-MgO	21.75	4.08
PP/ 10xGnP/2n-MgO	21.16	4.20

3.2. Microstructural investigation

The SEM micrographs of PP and its different xGnP and n-MgO composites are shown in Figure 2. The microstructure of the neat PP sample showed a wavy-like structure and this is a characteristic of the PP microstructure (Figure 2a). Moreover, Figures 2b to 2e presented the microstructures of the composites with various amounts of fillers, these are very important to justify the dispersion of fillers within the PP matrix. The microstructures of the

composites showed a good dispersion of fillers particles which were almost embedded into matrix and dispersed well and their interfaces are well bonded, which is expected to improve the mechanical properties of composites; however, little agglomerations were found in the composites samples with the addition of 5 and 10 wt.% xGnP as shown in Figures 2d and 2e, respectively. Although the xGnP is a potent filler, to achieve homogeneous dispersion remains the key challenge for effectively reinforcing the polymer, particularly for the non-polar polymer like polypropylene (PP) [24].

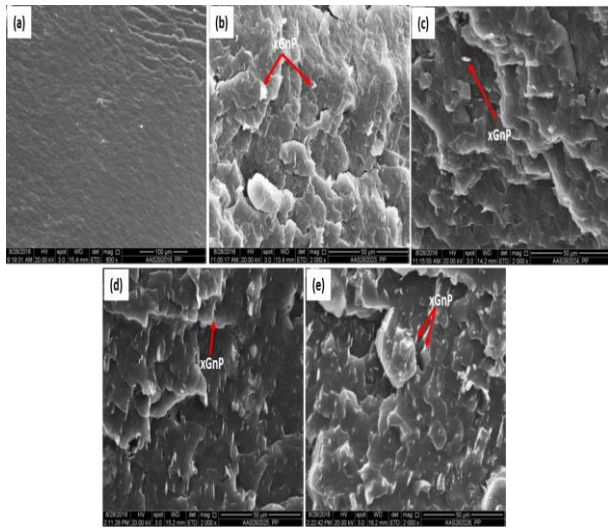


Fig. 2: SEM Images of PP and Its Composites: (A) 100 Wt. % PP, (B) PP/ 1xgnp/2n-Mgo, (C) PP/ 2.5xgnp/2n-Mgo, (D) PP/ 5xgnp/2n-Mgo and (E) PP/ 10xgnp/2n-Mgo.

3.3. Flexural strength

The average results of the flexural strength and flexural modulus of the different PP/xGnP/n-MgO composites are displayed in Figures 3 and 4, respectively. In addition, the average values of the composites flexural strength and flexural modulus are summarized in Table 4. As shown in Figure 3, a significant improvement in flexural strength of the composites were clearly depicted. Adding 1xGnP/2n-MgO to the PP resulted in increasing the flexural strength of the composite by ~ 18. Increasing the xGnP up to 10 wt. % revealed an increase in the flexural strength of the composite by ~ 35%. From these results, it can be understood that the addition of both fillers was effective to improve the flexural strength of the composites as can be seen in Figure 3. These increasing trends can be attributed to the high stiffness, uniform and homogeneous dispersion of xGnP and n-MgO in the polymer matrix as evidenced by XRD patterns and morphological images in Figs. 1 and 2, respectively. Accordingly, this improvement can be explained by the load transferred from matrix to reinforcement, as a consequence of adequate matrix-reinforcement adhesion. A similar trend had been revealed for the flexural modulus. Increasing the xGnP up to 10 wt. % revealed an increase in the flexural modulus of the composite by ~ 91. The development of flexural properties was attributed to the high aspect ratio of surface of fillers, that caused high interfacial interaction within the polymer matrix. Hence, it could be correlated to the load transferred from matrix to reinforcement, as a consequence of adequate matrix-reinforcement adhesion [26]. Other probable reason for the occurred enhancement could be relevant to the fact of adding stiff nanofillers to the neat matrix, which would lead to ameliorating the composite's modulus. Furthermore, constraints on movement of matrix chains under load are taken place when adopting the nanofillers; consequently, the flexural modulus was periodically increased. Also, the matrix chains' direction in accordance to the load orientation could be an important aspect for flexural modulus enhancement [22]. Additionally, the enhancement of flexural modulus may also be attributed to the alignment of xGnP and n-

MgO nanofillers to direction of flow during extrusion and injection molding cycles [27]

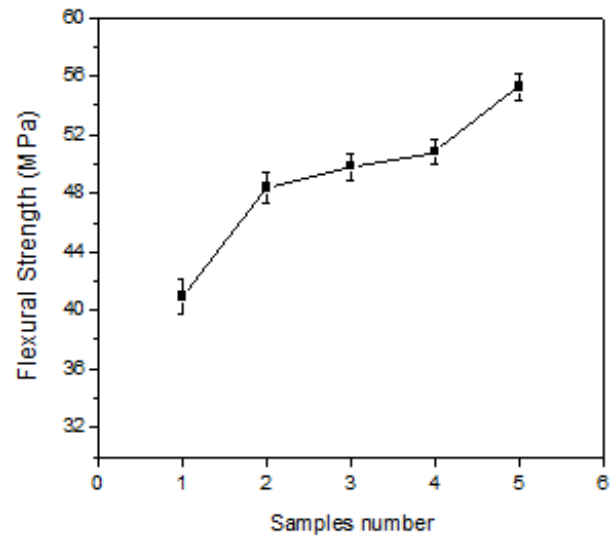


Fig. 3: Flexural Strength of the Neat PP and Its Composites.

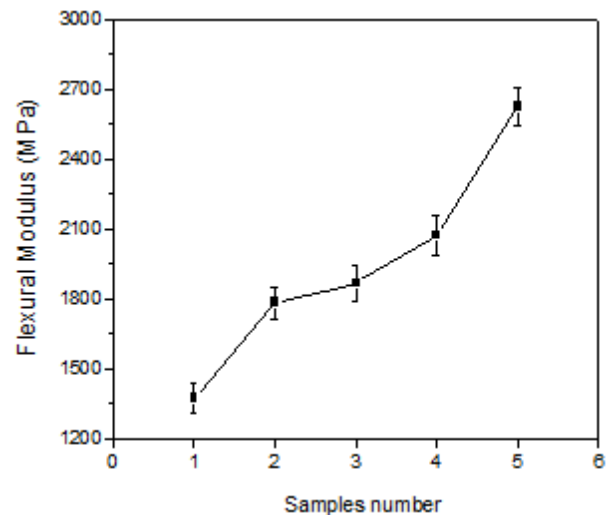


Fig. 4: Flexural Modulus of the Neat PP and their Composites.

Table 4: The Summary of Flexural Strength and Flexural Modulus of the Neat PP and Its Composites

Samples	Flexural strength (MPa)	Flexural Modulus (MPa)
100 wt. % PP	40.96	1373
PP/ 1xGnP/2n-MgO	48.38	1783
PP/ 2.5xGnP/2n-MgO	49.82	1866
PP/ 5xGnP/2n-MgO	50.8	2071
PP/ 10xGnP/2n-MgO	55.26	2626

3.4. Hardness measurement

Figure 5 shows the variation in hardness values of the composites with different amounts of fillers. In general, the hardness values of the composites were higher compared to the neat PP sample, this is due to the significant influence of the addition of the fillers into the PP matrix. As shown in Figure 5, a significant improvement in hardness values of the composites were clearly depicted. Adding 1xGnP/2n-MgO to the PP resulted in increasing the hardness of the composite by ~ 6.7%. Increasing the xGnP up to 10 wt. % revealed an increase in the flexural strength of the composite by ~ 10%.

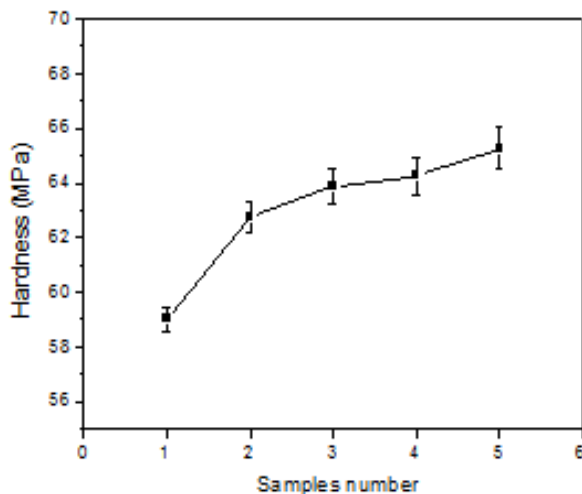


Fig. 5: Variation in Hardness Values of the Neat PP and Its Composites.

3.5. Fracture surface of the composites

Figure 6 shows the fracture surface of the neat PP and the composite with the addition of 5 wt.% xGnP. The neat PP demonstrated a typical ductile fracture as shown in Figure 6a. On the other hand, Figure 6b did not show the ductile morphology as a typical of PP, however, the surface fracture of the composite with 5 wt.% xGnP shows a brittle morphology. It confirmed that the addition of fillers could improve the strength of the composites which can be identified from its fracture surface morphology as shown in Figure 6b. In addition, the presence of n-MgOs was identified as white fine dots as presented in Figure 6b.

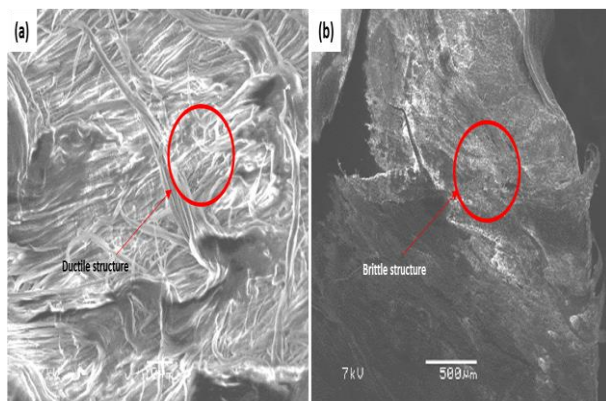


Fig. 6: The Fracture Surface of (A) the Neat PP and (B) the Composite with 5 Wt.% Xgnp.

4. Conclusion

The PP/xGnP/n-MgO composites were successfully fabricated, using injection molding machine. The present results showed that the combination of xGnP and n-MgO filler provided various results, showing remarkable improvement in the mechanical properties of composites. Generally, all the composites samples revealed better flexural strength, flexural modulus and hardness, if compared to the neat PP, which confirms that the addition of different types of fillers successfully improves the mechanical properties of the composites. The best compositions of composites were found in samples 5 where the gradual incorporation of xGnPs, led to excellent combination resulting in ameliorated mechanical properties. This improvement is attributed to the load transferred from matrix to reinforcement, as a consequence of adequate matrix-reinforcement adhesion.

5. Acknowledgement

The authors would like to thank and appreciate the effort of SABIC for their assistantship and tremendous help and contribution in the preparation of composites and its characterizations.

References

- [1] N. Zhao, H. Rödel, C. Herzberg, S.-L. Gao, and S. Krzywinski, "Stitched glass/PP composite. Part I: Tensile and impact properties," *Composites Part A: Applied Science and Manufacturing*, vol. 40, no. 5, pp. 635-643, 2009. <https://doi.org/10.1016/j.compositesa.2009.02.019>.
- [2] M. Tufail, "Processing investigation and optimization for hybrid thermoplastic composites," *Journal of University of Science and Technology Beijing, Mineral, Metallurgy, Material*, vol. 14, no. 2, pp. 185-189, 2007. [https://doi.org/10.1016/S1005-8850\(07\)60036-X](https://doi.org/10.1016/S1005-8850(07)60036-X).
- [3] C. Chuai, K. Almdal, L. Poulsen, and D. Plackett, "Conifer fibers as reinforcing materials for polypropylene-based composites," *Journal of Applied Polymer Science*, vol. 80, no. 14, pp. 2833-2841, 2001. <https://doi.org/10.1002/app.1400>.
- [4] C. Albano, J. Gonzalez, M. Ichazo, and D. Kaiser, "Thermal stability of blends of polyolefins and sisal fiber," *Polymer Degradation and Stability*, vol. 66, no. 2, pp. 179-190, 1999. [https://doi.org/10.1016/S0141-3910\(99\)00064-6](https://doi.org/10.1016/S0141-3910(99)00064-6).
- [5] A. Long, C. Wilks, and C. Rudd, "Experimental characterisation of the consolidation of a commingled glass/polypropylene composite," *Composites Science and Technology*, vol. 61, no. 11, pp. 1591-1603, 2001. [https://doi.org/10.1016/S0266-3538\(01\)00059-8](https://doi.org/10.1016/S0266-3538(01)00059-8).
- [6] A. Shalwan, A. Alateyah, B. Aldousiri, and M. Alajmi, "Thermal and Nanoindentation Behaviours of Layered Silicate Reinforced Recycled GF-12 Nanocomposites," *Journal of Materials Science Research*, vol. 5, no. 4, p. 10, 2016. <https://doi.org/10.5539/jmsr.v5n4p10>.
- [7] H. M. Da Costa, V. D. Ramos, and M. C. Rocha, "Analysis of thermal properties and impact strength of PP/SRT, PP/EPDM and PP/SRT/EPDM mixtures in single screw extruder," *Polymer Testing*, vol. 25, no. 4, pp. 498-503, 2006. <https://doi.org/10.1016/j.polymertesting.2006.02.003>.
- [8] T. Gong, S.-P. Peng, R.-Y. Bao, W. Yang, B.-H. Xie, and M.-B. Yang, "Low percolation threshold and balanced electrical and mechanical performances in polypropylene/carbon black composites with a continuous segregated structure," *Composites Part B: Engineering*, vol. 99, pp. 348-357, 2016. <https://doi.org/10.1016/j.compositesb.2016.06.031>.
- [9] P. Vilímová, J. Tokarský, P. Peikertová, K. M. Kutláková, and T. Plaček, "Influence of thermal and UV treatment on the polypropylene/graphite composite," *Polymer Testing*, vol. 52, pp. 46-53, 2016. <https://doi.org/10.1016/j.polymertesting.2016.03.025>.
- [10] L. Zhang, M. Kai, and K. Liew, "Evaluation of microstructure and mechanical performance of CNT-reinforced cementitious composites at elevated temperatures," *Composites Part A: Applied Science and Manufacturing*, vol. 95, pp. 286-293, 2017. <https://doi.org/10.1016/j.compositesa.2017.02.001>.
- [11] D. Pedrazzoli, A. Pegoretti, and K. Kalaitzidou, "Synergistic effect of exfoliated graphite nanoplatelets and short glass fiber on the mechanical and interfacial properties of epoxy composites," *Composites Science and Technology*, vol. 98, pp. 15-21, 2014. <https://doi.org/10.1016/j.compscitech.2014.04.019>.
- [12] S. N. Alam and L. Kumar, "Mechanical properties of aluminium based metal matrix composites reinforced with graphite nanoplatelets," *Materials Science and Engineering: A*, vol. 667, pp. 16-32, 2016. <https://doi.org/10.1016/j.msea.2016.04.054>.
- [13] M. Karevan, S. Eshraghi, R. Gerhardt, S. Das, and K. Kalaitzidou, "Effect of processing method on the properties of multifunctional exfoliated graphite nanoplatelets/polyamide 12 composites," *Carbon*, vol. 64, pp. 122-131, 2013. <https://doi.org/10.1016/j.carbon.2013.07.043>.
- [14] Y. Li, H. Zhang, H. Porwal, Z. Huang, E. Bilotti, and T. Peijs, "Mechanical, electrical and thermal properties of in-situ exfoliated graphene/epoxy nanocomposites," *Composites Part A: Applied Science and Manufacturing*, vol. 95, pp. 229-236, 2017. <https://doi.org/10.1016/j.compositesa.2017.01.007>.
- [15] F. Wang, L. T. Drzal, Y. Qin, and Z. Huang, "Enhancement of fracture toughness, mechanical and thermal properties of rubber/epoxy composites by incorporation of graphene nanoplatelets," *Composites Part A: Applied Science and*

- Manufacturing*, vol. 87, pp. 10-22, 2016. <https://doi.org/10.1016/j.compositesa.2016.04.009>.
- [16] T. Rath and Y. Li, "Nanocomposites based on polystyrene-b-poly(ethylene-r-butylene)-b-polystyrene and exfoliated graphite nanoplates: effect of nanoplatelet loading on morphology and mechanical properties," *Composites Part A: Applied Science and Manufacturing*, vol. 42, no. 12, pp. 1995-2002, 2011. <https://doi.org/10.1016/j.compositesa.2011.09.002>.
- [17] D. Chung, "Review graphite," *Journal of materials science*, vol. 37, no. 8, pp. 1475-1489, 2002. <https://doi.org/10.1023/A:1014915307738>.
- [18] K. Kalaitzidou, H. Fukushima, and L. T. Drzal, "A new compounding method for exfoliated graphite-polypropylene nanocomposites with enhanced flexural properties and lower percolation threshold," *Composites Science and Technology*, vol. 67, no. 10, pp. 2045-2051, 2007. <https://doi.org/10.1016/j.compscitech.2006.11.014>.
- [19] S. Kim, J. Seo, and L. T. Drzal, "Improvement of electric conductivity of LLDPE based nanocomposite by paraffin coating on exfoliated graphite nanoplatelets," *Composites Part A: Applied Science and Manufacturing*, vol. 41, no. 5, pp. 581-587, 2010. <https://doi.org/10.1016/j.compositesa.2009.05.002>.
- [20] M. Mantilaka, H. Pitawala, D. Karunaratne, and R. Rajapakse, "Nanocrystalline magnesium oxide from dolomite via poly(acrylate) stabilized magnesium hydroxide colloids," *Colloids and Surfaces A: Physicochemical and Engineering Aspects*, vol. 443, pp. 201-208, 2014. <https://doi.org/10.1016/j.colsurfa.2013.11.020>.
- [21] H. Abdizadeh, R. Ebrahimi-fard, and M. A. Baghchesara, "Investigation of microstructure and mechanical properties of nano MgO reinforced Al composites manufactured by stir casting and powder metallurgy methods: A comparative study," *Composites Part B: Engineering*, vol. 56, pp. 217-221, 2014. <https://doi.org/10.1016/j.compositesb.2013.08.023>.
- [22] A. I. Alateyah, H. N. Dhakal, and Z. Y. Zhang, "Processing, Properties, and Applications of Polymer Nanocomposites Based on Layer Silicates: A Review " *Advances in Polymer Technology*, vol. 32, no. 4, 2013. <https://doi.org/10.1002/adv.21368>.
- [23] Y. Geng, S. J. Wang, and J.-K. Kim, "Preparation of graphite nanoplatelets and graphene sheets," *Journal of colloid and interface science*, vol. 336, no. 2, pp. 592-598, 2009. <https://doi.org/10.1016/j.jcis.2009.04.005>.
- [24] Pingan Song, Zhenhu Cao, Yuanzheng Cai, Liping Zhao, Zhengping Fang, Shenyuan Fu, " Fabrication of exfoliated graphene-based polypropylene nanocomposites with enhanced mechanical and thermal properties," *Polymer*, vol. 52, pp. 4001-4010, 2011. <https://doi.org/10.1016/j.polymer.2011.06.045>.
- [25] F. S. AlHumaidan, A. Hauser, M. S. Rana, H. M.S. Lababidi, M. Behbehani, "Changes in asphaltene structure during thermal cracking of residual oils: XRD study," *Fuel*, vol. 150, pp. 558-564, 2015. <https://doi.org/10.1016/j.fuel.2015.02.076>.
- [26] A. I. Alateyah, H. N. Dhakal, and Z. Y. Zhang, "Water absorption behaviour, mechanical and thermal properties of vinyl ester matrix nanocomposites based on layered silicate," *Polymer-Plastics Technology and Engineering*, vol. 53, pp. 1-17, 2014. <https://doi.org/10.1080/03602559.2013.844246>.
- [27] S. O. Han, M. Karevan, M. A. Bhuiyan, J. H. Park, and K. Kalaitzidou, " Effect of exfoliated graphite nanoplatelets on the mechanical and viscoelastic properties of poly(lactic acid) biocomposites reinforced with kenaf fibers", *Journal of Materials Science*, Vol. 47 (8), pp 3535-3543, 2012. <https://doi.org/10.1007/s10853-011-6199-8>.